



Published in final edited form as:

J Immunol. 2018 December 15; 201(12): 3750–3758. doi:10.4049/jimmunol.1801041.

Sialic Acid-Dependent Inhibition of T cells by Exosomal Ganglioside GD3 in Ovarian Tumor Microenvironments

Gautam N. Shenoy^{*}, Jenni Loyall^{*}, Charles S. Berenson^{*,†}, Raymond J. Kelleher Jr.^{*}, Vandana Iyer[‡], Sathy V. Balu-Iyer[‡], Kunle Odunsi[§], and Richard B. Bankert^{*}

^{*} Department of Microbiology and Immunology, Jacobs School of Medicine and Biomedical Sciences, University at Buffalo, Buffalo, New York

[†] Infectious Disease Division, Jacobs School of Medicine and Biomedical Sciences, University at Buffalo, and Department of Veteran Affairs, Western New York Health Care System, Buffalo, New York.

[‡] Department of Pharmaceutical Sciences, University at Buffalo, Buffalo, New York

[§] Department of Gynecologic Oncology, Roswell Park Comprehensive Cancer Center, Elm and Carlton Streets, Buffalo, New York

Abstract

The tumor microenvironment is rendered immunosuppressive by a variety of cellular and acellular factors, which represent potential cancer therapeutic targets. While exosomes isolated from ovarian tumor ascites fluids have been previously reported to induce a rapid and reversible T cell arrest, the factors present on or within exosomes that contribute to immunosuppression have not been fully defined. Here, we establish that GD3, a ganglioside expressed on the surface of exosomes isolated from human ovarian tumor ascites fluids, is causally linked to the functional arrest of T cells activated through their T cell receptor. This arrest is inhibited by antibody blockade of exosomal GD3 or by the removal of GD3⁺ exosomes. Empty liposomes expressing GD3 on the surface also inhibit the activation of T cells, establishing that GD3 contributes to the functional arrest of T cells, independent of factors present in exosomes. Finally, we demonstrate that the GD3-mediated arrest of the TCR activation is dependent upon sialic acid groups, since their enzymatic removal from exosomes or liposomes results in a loss of inhibitory capacity. Collectively, these data define GD3 as a potential immunotherapeutic target.

Keywords

Exosomes; Ganglioside GD3; T cells; ovarian tumors; ascites fluid

Corresponding Author: Dr. Richard B. Bankert, VMD. Ph.D., Mailing Address: 955 Main Street, Suite 5118, Buffalo, New York 14203. Phone: 716-829-2701 Fax: 716-829-2158 rbankert@buffalo.edu.

Conflict of Interest Statement: The authors declare no potential conflicts of interest.

INTRODUCTION:

Ovarian cancer patients are often diagnosed with cancer at an advanced stage of their disease resulting in poor overall survival. While tumor-specific T-cells are present in the microenvironment of ovarian tumors (1–3), multiple immune suppressive factors act to inhibit T-cell anti-tumor activity and render them hyporesponsive to activation. Further, fully functional T-cells derived from peripheral blood (4) and tumor-specific Chimeric Antigen receptor (CAR) T-cells (5) become functionally arrested following their entry into the tumor microenvironment. A combination of regulatory T cells, myeloid derived suppressor cells, immune suppressive dendritic cells, immune-inhibitory checkpoint molecules, as well as soluble inhibitory factors such as TGF- β , prostaglandins and adenosine have been reported to contribute to a blockade of the anti-tumor response in tumor microenvironments (6–11). Additionally, nano-sized extracellular vesicles (exosomes) present in tumor microenvironments contribute to multiple aspects of cancer pathogenesis including tumor invasion, escape from immune regulation and metastasis (12–14).

A comprehensive analysis of lipids expressed by exosomes identified over 500 individual lipids including sphingolipids, sterol lipids, glycerolipids and glycerophospholipids like alkyl ether-containing glycerophospholipids (15). Elevated levels of sphingolipids in the plasma and ascites fluids have been found in patients with advanced ovarian cancer (16). Cancer patients with high levels of gangliosides have a faster rate of disease progression and a decreased survival rate (17). Elevated levels of gangliosides in patients with renal cell carcinomas have been associated with multiple T-cell dysfunctions (18). One specific ganglioside, GD3, induces apoptosis of T-cells (19), and high levels of GD3 found in ovarian tumor ascites fluids can inhibit natural killer (NK) T (NKT) cell activation (20). These studies led us to explore whether GD3 plays a role in the ability of tumor-derived exosomes to inhibit T-cell activation.

While previous studies have established that exosomes present in tumors are immunosuppressive, all the regulatory factors on the exosomes have not been identified (21). We report here that exosomes expressing GD3 on their surface contribute to immunosuppression and that this ganglioside is causally linked to the functional arrest of T cells. Further, we establish that empty liposomes formulated with GD3 can directly inhibit the induced activation of T-cells. This inhibition is dependent on sialic acid residues, since desialylation of exosomes or liposomes results in a significant knockdown of the inhibitory capacity. These findings establish that GD3 present on exosomes in the tumor microenvironment directly suppresses T-cells (independent of other cells and/or the exosomal cargo). We conclude that GD3 and sialic acid molecules on exosomes represent potential viable therapeutic targets for enhancing the anti-tumor activity of quiescent T-cells in tumor microenvironments.

Materials and Methods:

Specimens:

Primary tumors and ascites fluids from Stage III or Stage IV ovarian cancer patients were received from the Roswell Park Cancer Institute (RPCI) Tissue Procurement Facility. All the

tumors obtained were high grade serous epithelial ovarian carcinomas. Experiments were done using cell-free ascites fluids that had been stored at -80°C . Normal donor peripheral blood was provided by the Flow and Image Cytometry Facility at RPCI. Normal donor peripheral blood lymphocytes (NDPBL) were obtained by monocyte depletion and Ficoll-Hypaque density separation. Cells were frozen and stored in liquid nitrogen until use, as previously reported (22, 23). All specimens were obtained under sterile conditions and using IRB approved protocols.

Reagents:

See supplementary table 1.

Purification of gangliosides:

Total lipids were extracted from samples of ovarian cancer ascites from three separate patients with chloroform: methanol (1:1-v/v) and sonication. Gangliosides were purified from the total lipid extract as previously described (24). In brief, ganglioside-containing acidic lipids were eluted through a 3 ml. column of DEAE-Sephadex A-25 (Sigma Chemical Co., St. Louis, MO), dried by rotary evaporation and hydrolyzed with 0.1 N NaOH at 37°C for 90 min. Samples were neutralized with 0.1 N HCl and desalted on a reverse phase silica gel column (SepPak, Waters Assoc., Waltham MA). Samples were applied to a 2–3 ml. column of Iatrobeads 6RS-8060 (Iatron Laboratories, Tokyo, Japan) in chloroform-methanol (85:15, v/v). After elution of less polar lipids, the total ganglioside fraction was eluted with chloroform-methanol (1:2, v/v), and dried by rotary evaporation.

Thin layer chromatography:

Purified gangliosides were run in one or two dimensions on TLC plates in chloroform-methanol-0.25% KCl (50:45:10) (Solvent 1) and, after rotating the TLC plate 90° counterclockwise, in chloroform-methanol-0.25% KCl in 2.5 N NH_4 in 0.25% aqueous KCl (50:40:10) (Solvent 2). TLC plates run in one dimension were run in Solvent 1. Distinct ganglioside peaks were visualized by heating the TLC plates to $92-94^{\circ}\text{C}$ after spraying with resorcinol reagent (24).

Sialidase degradation of gangliosides:

A mixture of mono- and di-sialogangliosides containing 5–10 μg sialic acid were incubated with *Clostridium perfringens* sialidase (2U/ml) (Sigma Chemical Co., St. Louis, MO) in 0.5 ml of 50mM sodium citrate-phosphate buffer, pH 5.5, at 37°C , for 2h, as previously described (25). A duplicate sample of equal quantity of gangliosides was incubated in buffer alone. Reactions were terminated by addition of 0.1 M NaOH, neutralized with 0.1 M HCl, desalted on SepPak (Waters Assoc., Milford, MA) columns and evaluated on TLC for hydrolytic products, with resorcinol. The presence of resorcinol-negative spots on sialidase-treated samples was confirmed on TLC's, by reversible staining with iodine vapor, prior to resorcinol spraying (25). Efficacy of enzymatic activity was determined with gangliosides with sialidase-susceptible external sialic acid residues (GM3, GD3, GD1a, GD1b) and gangliosides with sialidase-resistant internal sialic acid residues (GM1a, GM2), respectively (Matreya LLC, Pleasant Gap, PA).

Isolation of exosomes:

Ascites fluids were first centrifuged at $300 \times g$ to separate cells and large debris, followed by another round of centrifugation at $1150 \times g$ to remove smaller debris and membrane fragments. They were then diluted to 50% [with RPMI-1640 or phosphate buffered saline (PBS)], passed through a $0.22 \mu\text{m}$ PVDF filter (Millipore) and ultracentrifuged at $200,000 \times g$ for 90 min. The pellet was resuspended in RPMI-1640 + 1% HSA (for functional experiments) or PBS (for biophysical characterization).

Flow exometry:

300–500 μg of exosomes were attached to 100 μl of aldehyde/sulfate latex beads ($4 \mu\text{m}$; 4% w/v) and incubated overnight at 4°C on a rotator/mixer. Glycine was then added to a final concentration of 100 mM to saturate remaining free binding sites on the beads. The beads were then washed in PBS with 0.5% bovine serum albumin (BSA) and used for immunofluor staining.

Scanning Electron Microscopy:

For SEM studies, exosomes were loaded onto a membrane scaffold with a $0.1 \mu\text{m}$ nucleopore membrane (Whatman). The exosome embedded membranes were fixed with 2% glutaraldehyde at 4°C for 90 min. The fixative was washed off and the samples dried using 30%, 50%, 70%, 80%, 95% and 100% ethanol sequentially for 15 min each. The samples were then exchanged into 100% hexamethyldisilazane (HMDS) and air dried in a chemical fume hood. The specimens were coated with evaporated carbon and analyzed using Hitachi SU-70 FE-SEM (Hitachi), operated at 2.0 kV.

Exosome antibody array:

The identification of protein markers on the isolated exosomes was done using the commercially available Exo-Check exosome antibody array (System Biosciences Inc.) kit as described by the manufacturer. The membrane was developed with SuperSignal West Femto Maximum Sensitivity Substrate (Thermo Fisher Scientific) and analyzed using ChemiDoc

Depletion of GD3+ exosomes:

50 μg of anti-GD3 antibody (Genetex) or isotype control (mouse IgG, Caltag) was conjugated to 5 mg Dynabeads M-280 Tosylactivated (Life Technologies) according to manufacturer's instructions. The conjugated beads were incubated with exosomes with tilting and rotation for 1 hour at 4°C to capture GD3+ exosomes. The unbound (GD3-) exosomes were separated from the exosome-bead complex using a magnet (BD Biosciences)

T cell activation with antibodies to CD3 and CD28:

Antibodies were immobilized on maxisorb 12×75 mm tubes (Nunc) by incubating 0.1 μg of purified anti-CD3 (Bio \times Cell, clone OKT3) and 5 μg of purified anti-CD28 (Invitrogen, clone 10F3) in 500 μl of PBS, at 4°C overnight. PBL from normal donors were thawed, resuspended in RPMI-1640 + 1% human serum albumin, and 5×10^5 total cells were incubated in anti-CD3/anti-CD28 in coated tubes at $37^\circ\text{C}/5\% \text{CO}_2$ for the duration of activation.

Detection of NF κ B translocation following T cell activation:

After activation, the cells were attached to alcian blue coverslips in a humid chamber (10 min) and fixed in 2% formaldehyde in 1x PBS (40 min). The cells were then permeabilized and blocked with 30 μ g normal mouse IgG in 5% normal mouse serum in 1x PBS + 0.4% Triton X-100. This was followed by staining for intracellular CD3 for 20 minutes. After washing once with NGS block (5% normal goat serum in 1X PBS), the cells were incubated with 2 μ g/mL goat anti-mouse IgG-Alexa Fluor 568 for 15 minutes. This was followed by staining with purified rabbit anti-human NF κ B p65 in NGS block/perm for 1 hour. After washing twice with NGS block, the cells were incubated with 2 μ g/mL goat anti-rabbit IgG-Alexa Fluor 488 in 100 μ L NGS block/perm for 30 minutes. The cells were washed twice with NGS block and twice with 1X PBS before mounting the coverslips on glass slides with Vectashield Mounting Medium (Vector Laboratories, Burlingame). Cells were then observed on a Zeiss LSM 510 Confocal Microscope with at least 400 CD3+ cells counted per condition.

Detection of CD69 expression following T cell activation:

Human NDPBL were activated for 2h at 37°C with immobilized anti-human CD3/CD28 with or without ovarian ascites fluid-derived exosomes. The cells were then incubated for 18h in RPMI-1640 + 1% HSA at 37°C/5% CO₂ in the absence of stimulation or exosomes. For flow cytometry, the cells were labeled with the recommended amounts of fluorochrome-conjugated antibodies to CD3 and CD69 for 30 mins at 4°C. The cells were then washed with 2 mL of PBS. Sytox Red was added 15 min before flow cytometry at a final concentration of 5 nM to label the dead cells. The samples were acquired on an LSR Fortessa (BD Biosciences) flow cytometer and analyzed using FlowJo software (Tree Star Inc. OR).

Detection of intracellular IL-2 and IFN- γ expression following T cell activation:

Human NDPBL were activated for 6h at 37°C/5% CO₂ with immobilized anti-human CD3/CD28 in the presence of 1 μ L/mL GolgiStop (BD Biosciences) with or without exosomes. For flow cytometry, the cells were labeled with fluorochrome-conjugated antibody to CD3 for 30 mins at 4°C. The cells were then fixed and permeabilized with the fixation/permeabilization solution from the Cytotfix/Cytoperm kit (BD Biosciences) as described by the manufacturer and labeled with fluorochrome-conjugated antibodies to IL-2 and IFN- γ at 4°C for 30 min, washed, fluorescence emission acquired, and results analyzed as above.

Preparation of GD3 liposomes:

The GD3 containing liposomes were prepared using thin film method as described previously (26). Briefly, chloroform solutions of phosphatidylcholine (PC) and ganglioside GD3 (from bovine milk; Avanti Lipids Cat # 860060) were mixed in a molar ratio of 70:30 in a glass tube and the solvent was evaporated using a roto evaporator. The thin film thus obtained was further flushed with nitrogen to ensure that there was no residual solvent. The dried film was then re-suspended with 1X PBS and incubated at 37 °C for 5 minutes to form multi lamellar vesicles. The vesicles were sonicated for 5 minutes and were then extruded using 80 nm poly carbonate filter multiple times to form small unilamellar vesicles. The

liposomes were prepared with 2 mM of the respective lipids, and then were diluted to a final concentration of 0.25 mM, 0.5 mM or 1 mM in the activation experiment.

Sialidase treatment of exosomes:

Exosomes, in a volume of 250 μ l. were treated with 0.1U (= 0.8U/mL) sialidase (neuraminidase) from *Clostridium perfringens* type \times (Sigma) for 2h at 37°C. The volume was then made up to 1 mL with activation media (RPMI-1640 + 1% HSA).

Calculation of % inhibition and % knockdown:

These were calculated using the formulae:

$$\% \text{ Inhibition} = [1 - (\% \text{ activation with exosomes} / \% \text{ activation without exosomes})] \times 100$$

$$\% \text{ Knockdown of inhibition} = [1 - (\% \text{ inhibition in test group} / \% \text{ inhibition in control group})] \times 100$$

Statistics:

All statistics were calculated using Excel 2013 (Microsoft). Paired or unpaired Student's t test was applied to determine whether the differences between groups could be considered significant. A p value higher than 0.05 was not significant (NS) while *p < 0.05; **p < 0.01 and ***p < 0.001 were considered significant.

Results

Ovarian ascites fluid derived exosomes express ganglioside GD3 on their surface.

We have previously shown that factors present in human ovarian cancer ascites fluids induce a T cell signaling arrest (23). Preliminary analysis attributed most of the inhibition of the T-cell activation to lipids in the ascites fluid (27), and was followed by attempts to identify the different lipids present in the ascites fluids by extraction with hexane and isopropyl alcohol. Using this approach, we extracted both non-polar (cholesterol esters, triglycerides and free fatty acids) and polar (phospholipids and gangliosides) lipids from the samples (27). Further studies revealed that phosphatidylserine (PS), a glycerophospholipid abundant in extracellular vesicles isolated from ovarian tumor ascites fluids, is causally linked to exosome-mediated immunosuppression (27). Because several gangliosides have immune suppressive properties, the dominant gangliosides present in ovarian cancer ascites fluids were identified and investigated for their contribution to the arrest of the T cell activation. Analysis of ovarian cancer ascites gangliosides by two-dimensional thin layer chromatography (2-D-TLC) revealed two predominant ganglioside doublets (Figure 1A) that co-migrated with mono- and disialogangliosides GM3 and GD3 respectively, along with a few minor components. No variation in ganglioside profiles was seen among the three samples. Desialylation was determined by loss of resorcinol-positivity on TLC, and resorcinol-negative spots were detected by reversible staining with iodine vapor, prior to resorcinol spraying. Controls confirmed effective desialylation of GM3, GD3, GD1a and GD1b (external sialic acid residues), but not of GM2 and GM1 (internal sialic acid residues).

Ovarian cancer ascites fluid-derived gangliosides showed a complete loss of sialic acid residues, supporting the identity of the major ganglioside doublets as GM3 and GD3.

GD3 has been reported to be associated with multiple tumor types (19, 28–31) including ovarian tumors (20), and has been implicated in T cell and NKT cell dysfunction (18, 20). GD3 has also been reported to be present on exosomes in cancer patients (29). We have previously demonstrated the presence of immunosuppressive exosomes in ovarian tumor microenvironments (14, 27). These observations led us to investigate if GD3 was expressed on the surface of the exosomes and whether it contributed to exosome-associated arrest of the T cell function.

A scanning electron microscopic (SEM) analysis of the vesicles isolated from ovarian ascites fluids by ultracentrifugation as described previously (14, 27), revealed spherical membrane-bound vesicles with a modal diameter of 40–70 nm (Fig.S1A), consistent with published reports (14). Additionally, biochemical characterization using a commercially available antibody platform (Exosome Antibody Array) revealed the presence of exosomal marker proteins CD63, Flotillin-1, ICAM, EpCAM, Annexin V and TSG101 (Fig.S1B), confirming their identity as exosomes.

To determine if GD3 was expressed on the surface of ascites fluid-derived exosomes, the vesicles were first attached to latex beads and exosome-bound beads stained with anti-GD3 antibody followed by a fluorescently labeled secondary antibody. Flow cytometric analysis (Fig 1B) revealed that the exosome-bound latex beads stain positive for GD3 [mean fluorescence intensity (MFI) 804] over controls [unstained beads (MFI 104) or secondary antibody only (MFI 185)]. We tested exosomes derived from the ascites fluids of 11 different patients, and they were all found to express GD3 at different levels (Fig S2 and data not shown). For 8 of these patients, we also tested (EpCAM+) tumor cells derived from cryopreserved primary tumors for GD3 expression by flow cytometry. Although the expression levels varied from patient to patient, all the tumors tested were positive for surface expression of GD3 (Fig. S3A). We conclude that ovarian tumor cells as well as a significant proportion of the exosomes isolated from the tumor ascites fluids express GD3 on their surface.

Immunodepletion of GD3+ exosomes diminishes the inhibitory effect.

To determine if the GD3+ exosome subset contributes to the observed immunosuppression of T cells, we depleted GD3+ exosomes using magnetic beads coupled to an anti-GD3 antibody (or an antibody isotype control) and compared their inhibitory activity to an un-depleted preparation of exosomes. Cells were pulsed with a polyclonal activation stimulus, and the un-depleted or depleted fractions of exosomes for 2h, following which they were rested overnight. Activation was determined by detecting the upregulation of CD69 (a T cell activation associated event) on viable CD3+ T cells (Fig. 2A-C). As expected, over 90% of T cells upregulated CD69 when activated, and this upregulation was substantially inhibited (by 39%) by the exosomes (Fig. 2A-B). However, the removal of GD3+ exosomes from the heterogeneous vesicle population knocked down exosomal inhibition by 40%, while exosomes incubated with antibody isotype control magnetic beads minimally (5%) knocked down the inhibitory activity of the exosomes. These results are consistent with the

possibility that a subset of exosomes expressing GD3 on their surface contribute to the arrest of T-cell activation.

Antibody-mediated blockade of exosomal GD3 diminishes the inhibitory effect.

The exosome depletion experiments above demonstrate an association of the GD3 exosomes with the T cell arrest and suggest that the GD3⁺ exosomes are contributing to the T-cell suppression. However, it is possible that GD3 may simply be present on the inhibitory exosomes without playing an active role (i.e. being causally linked) to the induction of the T cell arrest. To determine if the ganglioside could be more closely associated with the functional arrest of T cells, we attempted to block exosomal immune suppression using an anti-GD3 antibody. Exosomes were pretreated with 10 µg of anti-GD3 antibody for 1 hour at 37°C. T cells were then activated with a polyclonal stimulus for 2h in the presence of untreated exosomes, anti-GD3 treated exosomes, or 10 µg anti-GD3 antibody only (no exosomes). The effect of these perturbations was assessed on an endpoint that has been unequivocally linked to an early functional activation event for T cells, i.e. the translocation of a transcription factor NFκB from the cytosol into the nucleus. Following the 2h activation without exosomes, over 60% of the T cells had translocated NFκB into the nucleus (Fig. 3). This level of activation was not altered by the presence of anti-GD3 antibody. As expected, there was a 50% inhibition of the NFκB translocation in the T cells activated in the presence of exosomes. This exosome-induced suppression of the translocation decreased from 50% to 26% (i.e. a 48% knockdown) when the T cells were activated with exosomes and anti-GD3 antibody (Fig. 3A).

Translocation of NFκB is an early activation event that precedes numerous downstream T cell functions including multiple cytokine production, degranulation, and proliferation. We have reported previously that exosomes derived from ovarian ascites fluids inhibit endpoints of T cell activation, including cytoplasmic expression of the cytokines IFN-γ and IL-2 (14). In view of this, we proceeded to test the effect of exosome blocking with anti-GD3 antibody on these two downstream activation endpoints. Consistent with previous studies, activation in the presence of untreated exosomes resulted in the inhibition of intracellular IFN-γ (77%) and IL-2 (75%) (Fig 3B-E). However, treatment of exosomes with anti-GD3 antibody was found to knockdown exosomal suppression of IFN-γ expression (by 58%) as well as IL-2 (by 64%) (Fig 3B-E). We conclude from these results that GD3 expressed on the surface of exosomes is directly contributing to the suppression of T cell activation.

GD3 expressed on the surface of liposomes acts directly and independently to inhibit the activation of T cells

We have previously established that immune suppressive exosomes bind to and are internalized by T cells (14). GD3 could serve as a ligand that binds to a T cell receptor facilitating exosomal internalization, enabling the release of one or more immunosuppressive factors, or could directly and independently arrest T cells. If the latter were true, empty vesicles expressing GD3 on the surface would arrest T cell function. To test this, we formulated liposomes expressing GD3 on their surface. Since liposomes that are formulated with 100% GD3 aggregate, we prepared liposomes that were 30% GD3 and 70% phosphatidylcholine (GD3/PC), which do not aggregate. 100% phosphatidylcholine (PC)

liposomes (that do not aggregate) were used as a control, since they have been shown to have no effect on T cell activation (27). The effect of these lipids at 0.25 mM, 0.5 mM or 1 mM (on liposomes) on T cells activated via the TCR or by bypassing the TCR (using PMA and ionomycin) was then determined. We observed that T cell activation was inhibited in a dose dependent manner by GD3/PC liposomes, but not PC only liposomes when activated through the TCR (Fig. 4A-B). This is consistent with our previous findings that exosome-mediated T cell arrest occurs proximal to the TCR and can be bypassed by activating using PMA/ionomycin (23, 27). Since the GD3/PC liposomes did not inhibit PMA/ionomycin activated cells even at the highest dose used (Fig. 4C), a non-specific lipid-mediated toxicity can be ruled out. Together, we conclude that vesicular GD3 acts by itself and is sufficient to induce the signature signaling arrest in T cells that is characteristic of exosome-mediated immunosuppression.

Sialidase treatment diminishes exosome-mediated functional arrest of T cells.

GD3 is a disialylated glycosphingolipid. Sialic acids can bind to sialic acid-binding Ig type lectins (Siglec) receptors, which have intracellular immunoreceptor tyrosine-based inhibitory motifs (ITIMs) that signal to downregulate T cell responses (32). Sialic acid-modified antigens can induce tolerance by inhibiting T cell proliferation and inducing T regulatory cells (33). We hypothesized that the sialic acid residues played a role in the observed immunosuppressive activity of GD3. To test this hypothesis, we treated exosomes with *C. perfringens* sialidase (25) to remove sialic acid residues and determined the inhibitory activity of these sialidase-treated exosomes on the activation of T cells using upregulation of CD69 as the activation endpoint. While sialidase by itself had no effect upon the activation of T cells, sialidase treatment of exosomes was found to knock down their ability to inhibit T cell activation by 42%, implicating a role for sialic acid residues in exosome-mediated immune suppression (Fig 5A-B).

Inhibitory activity of GD3 is sialic acid-dependent.

Since sialidase can target sialic acid groups on GD3 or other glycosylated molecules including proteins on the exosomal surface, the role of sialoglycoproteins in exosome-mediated immunosuppression cannot be ruled out. To determine whether sialic acid residues on GD3 are critical for the inhibition of T cells, we treated GD3/PC (30:70) liposomes with *C. perfringens* sialidase and compared their T cell inhibitory capacity with untreated liposomes. While GD3/PC liposomes inhibited T cell activation by 43%, this activation was brought down almost completely to 1.5% (97% knockdown) following their sialidase treatment (Fig 6). Since, GD3 is the only substrate for sialidase to act on in these liposomes, the near total knockdown of GD3 liposome-mediated T cell arrest following enzymatic treatment indicates the critical role of sialic acid residues on GD3 for inhibition. Thus, GD3-mediated inhibition of T cell activation is sialic acid-dependent.

Together, these results establish that sialic acid present on GD3 and possibly other glycoproteins on the exosome surface is causally linked to the arrest of the activation of T cells stimulated through the T cell receptor.

Discussion

Exosomes derived from ovarian ascites fluids have been shown to inhibit the activation of T cells rapidly and reversibly (14, 27). We have reported previously that phosphatidylserine, a glycerophospholipid abundant in extracellular vesicles isolated from ovarian tumor ascites fluids, is causally linked to exosome-mediated immunosuppression, and a blockade of PS using an anti-PS antibody or Annexin-V, or the removal of PS+ exosomes knocked down the exosome-mediated immunosuppression (27). The knockdown of inhibition observed in these experiments, in which PS+ exosomes were either blocked by using Annexin V or anti-PS antibodies or removed by immune-magnetic separation, was only partial and ranged from 40–50% (27). This suggested the presence of other factor(s) in or on exosomes that can inhibit T cells. In this study, we identify ganglioside GD3 as an inhibitory lipid present on exosomes derived from an ovarian tumor microenvironment that is causally linked to the immunosuppression of T cells. We further demonstrate that the inhibitory capacity of GD3 is directly dependent on sialic acid residues, and targeting either GD3 or the sialic acid residues is a viable approach to counter GD3-mediated immune suppression.

GD3 has been reported to be associated with multiple tumor types, including renal cell carcinomas (19, 28, 29), melanomas (30), neuroblastomas (31) and ovarian tumors (20). GD3 has also been detected in urinary exosomes in renal cell carcinoma patients (29) and has been reported to be associated with T cell dysfunction (18). Interestingly, GD3 is also expressed on the surface of resting memory T cells (34) and is upregulated in naïve T cells following their activation (35). We confirm here that GD3 is present in ovarian tumor ascites fluids, and report its abundance in exosomes derived from these fluids. We also report the expression of GD3 on the surface of ovarian tumor cells as well as tumor-infiltrating T cells from primary tumors (Fig. S3B). Tumor-associated exosomes derived from ovarian tumor ascites fluids have been shown to be a heterogeneous population that originate from a variety of different cell types, including tumor cells. GD3+ exosomes could therefore originate from tumor cells as well as tumor-associated T cells, with the latter possibly being a feedback immune-regulatory mechanism. Since the inhibitory activity of tumor-associated exosomes has been correlated to their binding and internalization by T cells (14), GD3 on exosomal surface may potentially play a different immunosuppressive role from GD3 expressed on the surface of tumor cells. Further studies on whether binding and internalization of GD3+ exosomes is necessary for their immunosuppressive activity will provide clearer insights.

Pre-activated T cells when exposed to GD3 for long periods (24–72h), internalize the ganglioside and undergo mitochondrial permeability transition, degradation of anti-apoptotic proteins, and ultimately, apoptosis (19). Long-term exposure to GD3 has also been known to lead to degradation of the NF κ B components RelA and p50 via a caspase-dependent pathway in peripheral blood-derived T cells and Jurkat cells (36).

We have shown previously that exosomes derived from ovarian tumor ascites fluids can inhibit T cell activation through the TCR rapidly, within 2h (14, 27). This inhibition can be overcome by using PMA, an analog of diacylglycerol - a key intermediate in the signaling pathway downstream of the TCR (27). We find here that the TCR signaling arrest mediated by GD3+ liposomes is consistent with this pattern. Further the inhibition that follows a brief

2h exposure to exosomes is not associated with cell death and is reversible, since the removal of exosomes renders the T cells activatable. The inhibition experiments reported here are also done with 2h exposure to exosomes (or liposomes), which rules out the long term effects of T cell exposure to GD3 such as the induction of apoptosis through mitochondrial permeability alteration.

While there are multiple reports about the immunosuppressive nature of exosomes in different microenvironments, these studies have focused mostly on exosomal cargo such as inhibitory proteins and miRNAs as the primary mechanisms of inhibition (21). However, it is becoming increasingly clear that lipids expressed on the exosomal surface play an important role in exosome-mediated immunosuppression [(27) and current study]. By using liposomes that have lipids on their surface, but no cargo, we have now identified 2 lipids – PS and ganglioside GD3 on the exosome surface that are causally linked to T cell arrest. Since this arrest is rapid i.e. occurring within 2h of exposure to the lipids, it is unlikely to involve substantial transcriptional modulation in T cells.

We demonstrate here that the removal of sialic acid groups from exosomes by sialidase treatment is seen to result in a partial knockdown of their suppressive activity. Since sialidase can target sialic acid groups on GD3 or other glycosylated molecules including proteins on the exosomal surface, the role of other sialic acid-containing molecules in exosome-mediated immunosuppression cannot be ruled out. However, when the PC/GD3 liposomes are treated, GD3 is the only available substrate for sialidase to act upon, and therefore the finding that there is a near total knockdown of GD3 liposome-mediated T cell arrest following enzymatic treatment supports the fact that sialic acid residues on GD3 are necessary and sufficient to mediate the inhibition of T cell activation.

Sialic acids can bind to sialic acid-binding Ig type lectin (Siglec) receptors, which have intracellular immunoreceptor tyrosine-based inhibitory motifs (ITIMs) (32). Signaling through these motifs result in downregulation of T cell responses. Sialic acid-modified antigens have been reported to induce tolerance by inhibiting T cell proliferation and inducing T regulatory cells (33). By virtue of its sialic acid groups, GD3 can bind to multiple Siglecs (37), of which Siglec-7 and Siglec-9 are expressed on T cells (38, 39). These represent putative mechanisms for the observed immunosuppressive activity of GD3+ exosomes that warrant further investigation. There have been efforts to reverse immunosuppression by targeting the sialic acid-Siglec interactions (40). Additionally, GD3 has been used as an immunotherapy target for melanomas (41–45). The anti-GD3 antibody used in our study (clone R24) has been used by itself, or in combination with IL-2 in various clinical trials over the last two decades. Typical patient responses that were observed in these studies included increases in number of lymphocytes (43, 44), T cell activation (44), and antibody-dependent cellular cytotoxicity (41, 43). In the context of our finding that exosomal GD3 can suppress T cell function following a brief exposure, as well as reports from other investigators that have demonstrated induction of apoptosis in T cells following longer exposures to GD3 (19), increased numbers and function of lymphocytes that are observed in these clinical trials targeting GD3 are expected findings.

First and second generation CAR T cells have been designed against GD3 and tested against melanoma cells (46, 47). While these T cells recognized and killed GD3+ melanoma cells efficiently *in vitro*, they failed to suppress tumor growth in a mouse model of melanoma unless IL-2 was co-administered (46). These results are consistent with the notion that GD3 in tumor microenvironments inhibit T cell function. GD3+ exosomes can affect the CAR T cells in two possible ways. They can either compete with GD3 on melanoma cell surface for binding to the CAR T cells, thereby reducing their efficacy. The GD3+ exosomes could also functionally inhibit CAR T cells following their binding and internalization. It is reasonable to predict that combining strategies that block or overcome exosomal immunosuppression in combination with CAR T cells in future would enhance their efficacy.

Our findings reveal that exosomal GD3 is linked to T cell arrest and therefore represents a potential therapeutic target in ovarian tumor microenvironments. The fact that experiments involving blocking or depleting GD3+ exosomes knocked down only part of the inhibition suggests the presence of other immunosuppressive mechanisms associated with these exosomes. Nevertheless, the data presented here lay the foundation and provide a solid rationale for subsequent *in vivo* studies. While beyond the scope of the current study, *in vivo* testing in a suitable animal model will determine whether GD3+ exosomes represent a T cell checkpoint (that is a viable therapeutic target) that is able to suppress T cell control of tumors. We are currently in the process of developing and evaluating a tumor xenograft model that will enable us to carry out these studies. Devising efficient means to block GD3 to enhance the ability of the tumor-specific T cells to suppress or completely eradicate tumors and prevent their subsequent metastasis will be critical in determining their potential as effective targets for cancer therapy.

Supplementary Material

Refer to Web version on PubMed Central for supplementary material.

ACKNOWLEDGEMENTS:

The authors thank Anthony Miliotto and the Tissue Procurement Facility of RPCI for their assistance in providing ascites fluid. Flow cytometry and confocal microscopy services were provided by the Confocal Microscopy and Flow Cytometry Core Facility at the University at Buffalo. Electron microscopy services were provided by Mr. Peter J. Bush at the Electron Microscopy Core Facility at the University at Buffalo.

Financial Support: Research reported in this article was supported by the National Cancer Institute of the NIH under award numbers R01CA108970 and R01CA131407 (to R.B. Bankert), the National Heart, Lung, and Blood Institute of the NIH under award number R01HL70227 (to S. Balu-Iyer), and the NIH under award numbers P50CA159981 and R01CA158318 (to K. Odunsi).

References

1. Santin AD, Bellone S, Ravaggi A, Pecorelli S, Cannon MJ, and Parham GP 2000 Induction of ovarian tumor-specific CD8+ cytotoxic T lymphocytes by acid-eluted peptide-pulsed autologous dendritic cells. *Obstet Gynecol* 96: 422–430. [PubMed: 10960637]
2. Ramakrishna V, Ross MM, Petersson M, Gatlin CC, Lyons CE, Miller CL, Myers HE, McDaniel M, Karns LR, Kiessling R, Parmiani G, and Flyer DC 2003 Naturally occurring peptides associated with HLA-A2 in ovarian cancer cell lines identified by mass spectrometry are targets of HLA-A2-restricted cytotoxic T cells. *Int Immunol* 15: 751–763. [PubMed: 12750359]

3. Zhang L, Conejo-Garcia JR, Katsaros D, Gimotty PA, Massobrio M, Regnani G, Makrigiannakis A, Gray H, Schlienger K, Liebman MN, Rubin SC, and Coukos G 2003 Intratumoral T cells, recurrence, and survival in epithelial ovarian cancer. *N Engl J Med* 348: 203–213. [PubMed: 12529460]
4. Yokota SJ, Facciponte JG, Kelleher RJ, Jr., Shultz LD, Loyall JL, Parsons RR, Odunsi K, Frelinger JG, Lord EM, Gerber SA, Balu-Iyer SV, and Bankert RB 2013 Changes in ovarian tumor cell number, tumor vasculature, and T cell function monitored in vivo using a novel xenograft model. *Cancer Immunol* 13: 11. [PubMed: 23885217]
5. Moon EK, Wang LC, Dolfi DV, Wilson CB, Ranganathan R, Sun J, Kapoor V, Scholler J, Pure E, Milone MC, June CH, Riley JL, Wherry EJ, and Albelda SM 2014 Multifactorial T-cell hypofunction that is reversible can limit the efficacy of chimeric antigen receptor-transduced human T cells in solid tumors. *Clin Cancer Res* 20: 4262–4273. [PubMed: 24919573]
6. Huarte E, Cubillos-Ruiz JR, Nesbeth YC, Scarlett UK, Martinez DG, Buckanovich RJ, Benencia F, Stan RV, Keler T, Sarobe P, Sentman CL, and Conejo-Garcia JR 2008 Depletion of dendritic cells delays ovarian cancer progression by boosting antitumor immunity. *Cancer Res* 68: 7684–7691. [PubMed: 18768667]
7. Cubillos-Ruiz JR, Rutkowski M, and Conejo-Garcia JR 2010 Blocking ovarian cancer progression by targeting tumor microenvironmental leukocytes. *Cell Cycle* 9: 260–268. [PubMed: 20023378]
8. Landskron J, Helland O, Torgersen KM, Aandahl EM, Gjertsen BT, Bjorge L, and Tasken K 2015 Activated regulatory and memory T-cells accumulate in malignant ascites from ovarian carcinoma patients. *Cancer Immunol Immunother* 64: 337–347. [PubMed: 25416072]
9. Scarlett UK, Cubillos-Ruiz JR, Nesbeth YC, Martinez DG, Engle X, Gewirtz AT, Ahonen CL, and Conejo-Garcia JR 2009 In situ stimulation of CD40 and Toll-like receptor 3 transforms ovarian cancer-infiltrating dendritic cells from immunosuppressive to immunostimulatory cells. *Cancer Res* 69: 7329–7337. [PubMed: 19738057]
10. Scarlett UK, Rutkowski MR, Rauwerdink AM, Fields J, Escovar-Fadul X, Baird J, Cubillos-Ruiz JR, Jacobs AC, Gonzalez JL, Weaver J, Fiering S, and Conejo-Garcia JR 2012 Ovarian cancer progression is controlled by phenotypic changes in dendritic cells. *J Exp Med* 209: 495–506. [PubMed: 22351930]
11. Goynes HE, Stone PJ, Burnett AF, and Cannon MJ 2014 Ovarian tumor ascites CD14+ cells suppress dendritic cell-activated CD4+ T-cell responses through IL-10 secretion and indoleamine 2,3-dioxygenase. *J Immunother* 37: 163–169. [PubMed: 24598451]
12. Robbins PD, and Morelli AE 2014 Regulation of immune responses by extracellular vesicles. *Nat Rev Immunol* 14: 195–208. [PubMed: 24566916]
13. Taylor DD, and Gercel-Taylor C 2011 Exosomes/microvesicles: mediators of cancer-associated immunosuppressive microenvironments. *Semin Immunopathol* 33: 441–454. [PubMed: 21688197]
14. Shenoy GN, Loyall J, Maguire O, Iyer V, Kelleher RJ, Jr., Minderman H, Wallace PK, Odunsi K, Balu-Iyer SV, and Bankert RB 2018 Exosomes Associated with Human Ovarian Tumors Harbor a Reversible Checkpoint of T-cell Responses. *Cancer Immunol Res* 6: 236–247. [PubMed: 29301753]
15. Lydic TA, Townsend S, Adda CG, Collins C, Mathivanan S, and Reid GE 2015 Rapid and comprehensive ‘shotgun’ lipid profiling of colorectal cancer cell derived exosomes. *Methods* 87: 83–95. [PubMed: 25907253]
16. Santin AD, Ravindranath MH, Bellone S, Muthugounder S, Palmieri M, O’Brien TJ, Roman J, Cannon MJ, and Pecorelli S 2004 Increased levels of gangliosides in the plasma and ascitic fluid of patients with advanced ovarian cancer. *BJOG* 111: 613–618. [PubMed: 15198791]
17. Valentino L, Moss T, Olson E, Wang HJ, Elashoff R, and Ladisch S 1990 Shed tumor gangliosides and progression of human neuroblastoma. *Blood* 75: 1564–1567. [PubMed: 2317562]
18. Biswas S, Biswas K, Richmond A, Ko J, Ghosh S, Simmons M, Rayman P, Rini B, Gill I, Tannenbaum CS, and Finke JH 2009 Elevated levels of select gangliosides in T cells from renal cell carcinoma patients is associated with T cell dysfunction. *J Immunol* 183: 5050–5058. [PubMed: 19801523]

19. Sa G, Das T, Moon C, Hilston CM, Rayman PA, Rini BI, Tannenbaum CS, and Finke JH 2009 GD3, an overexpressed tumor-derived ganglioside, mediates the apoptosis of activated but not resting T cells. *Cancer Res* 69: 3095–3104. [PubMed: 19276353]
20. Webb TJ, Li X, Giuntoli RL, 2nd, Lopez PH, Heuser C, Schnaar RL, Tsuji M, Kurts C, Oelke M, and Schneck JP 2012 Molecular identification of GD3 as a suppressor of the innate immune response in ovarian cancer. *Cancer Res* 72: 3744–3752. [PubMed: 22649190]
21. Whiteside TL 2016 Exosomes and tumor-mediated immune suppression. *J Clin Invest* 126: 1216–1223. [PubMed: 26927673]
22. Broderick L, Brooks SP, Takita H, Baer AN, Bernstein JM, and Bankert RB 2006 IL-12 reverses anergy to T cell receptor triggering in human lung tumor-associated memory T cells. *Clin Immunol* 118: 159–169. [PubMed: 16271513]
23. Simpson-Abelson MR, Loyall JL, Lehman HK, Barnas JL, Minderman H, O'Loughlin KL, Wallace PK, George TC, Peng P, Kelleher RJ, Jr., Odunsi K, and Bankert RB 2013 Human ovarian tumor ascites fluids rapidly and reversibly inhibit T cell receptor-induced NF-kappaB and NFAT signaling in tumor-associated T cells. *Cancer Immun* 13: 14. [PubMed: 23882159]
24. Berenson CS, Nawar HF, Kruzel RL, Mandell LM, and Connell TD 2013 Ganglioside-binding specificities of *E. coli* enterotoxin LT-IIc: Importance of long-chain fatty acyl ceramide. *Glycobiology* 23: 23–31. [PubMed: 22917572]
25. Berenson CS, Nawar HF, Yohe HC, Castle SA, Ashline DJ, Reinhold VN, Hajishengallis G, and Connell TD 2010 Mammalian cell ganglioside-binding specificities of *E. coli* enterotoxins LT-IIb and variant LT-IIb(T13I). *Glycobiology* 20: 41–54. [PubMed: 19749203]
26. Gaitonde P, Ramakrishnan R, Chin J, Kelleher RJ, Jr., Bankert RB, and Balu-Iyer SV 2013 Exposure to factor VIII protein in the presence of phosphatidylserine induces hypo-responsiveness toward factor VIII challenge in hemophilia A mice. *J Biol Chem* 288: 17051–17056. [PubMed: 23649621]
27. Kelleher RJ, Jr., Balu-Iyer S, Loyall J, Sacca AJ, Shenoy GN, Peng P, Iyer V, Fathallah AM, Berenson CS, Wallace PK, Tario J, Odunsi K, and Bankert RB 2015 Extracellular Vesicles Present in Human Ovarian Tumor Microenvironments Induce a Phosphatidylserine-Dependent Arrest in the T-cell Signaling Cascade. *Cancer Immunol Res* 3: 1269–1278. [PubMed: 26112921]
28. Biswas K, Richmond A, Rayman P, Biswas S, Thornton M, Sa G, Das T, Zhang R, Chahlavi A, Tannenbaum CS, Novick A, Bukowski R, and Finke JH 2006 GM2 expression in renal cell carcinoma: potential role in tumor-induced T-cell dysfunction. *Cancer Res* 66: 6816–6825. [PubMed: 16818659]
29. Del Boccio P, Raimondo F, Pieragostino D, Morosi L, Cozzi G, Sacchetta P, Magni F, Pitto M, and Urbani A 2012 A hyphenated microLC-Q-TOF-MS platform for exosomal lipidomics investigations: application to RCC urinary exosomes. *Electrophoresis* 33: 689–696. [PubMed: 22451062]
30. Ritter G, and Livingston PO 1991 Ganglioside antigens expressed by human cancer cells. *Semin Cancer Biol* 2: 401–409. [PubMed: 1810468]
31. Ladisch S, and Wu ZL 1985 Detection of a tumour-associated ganglioside in plasma of patients with neuroblastoma. *Lancet* 1: 136–138. [PubMed: 2857215]
32. Crocker PR, Paulson JC, and Varki A 2007 Siglecs and their roles in the immune system. *Nat Rev Immunol* 7: 255–266. [PubMed: 17380156]
33. Perdicchio M, Ilarregui JM, Verstege MI, Cornelissen LA, Schetters ST, Engels S, Ambrosini M, Kalay H, Veninga H, den Haan JM, van Berkel LA, Samsom JN, Crocker PR, Sparwasser T, Berod L, Garcia-Vallejo JJ, van Kooyk Y, and Unger WW 2016 Sialic acid-modified antigens impose tolerance via inhibition of T-cell proliferation and de novo induction of regulatory T cells. *Proc Natl Acad Sci U S A* 113: 3329–3334. [PubMed: 26941238]
34. Merritt WD, Taylor BJ, Der-Minassian V, and Reaman GH 1996 Coexpression of GD3 ganglioside with CD45RO in resting and activated human T lymphocytes. *Cell Immunol* 173: 131–148. [PubMed: 8871609]
35. Villanueva-Cabello TM, Mollicone R, Cruz-Munoz ME, Lopez-Guerrero DV, and Martinez-Duncker I 2015 Activation of human naive Th cells increases surface expression of GD3 and

- induces neoexpression of GD2 that colocalize with TCR clusters. *Glycobiology* 25: 1454–1464. [PubMed: 26263924]
36. Thornton MV, Kudo D, Rayman P, Horton C, Molto L, Cathcart MK, Ng C, Paszkiewicz-Kozik E, Bukowski R, Derweesh I, Tannenbaum CS, and Finke JH 2004 Degradation of NF-kappa B in T cells by gangliosides expressed on renal cell carcinomas. *J Immunol* 172: 3480–3490. [PubMed: 15004148]
 37. Rapoport E, Mikhalyov I, Zhang J, Crocker P, and Bovin N 2003 Ganglioside binding pattern of CD33-related siglecs. *Bioorg Med Chem Lett* 13: 675–678. [PubMed: 12639556]
 38. Nicoll G, Ni J, Liu D, Klenerman P, Munday J, Dubock S, Mattei MG, and Crocker PR 1999 Identification and characterization of a novel siglec, siglec-7, expressed by human natural killer cells and monocytes. *J Biol Chem* 274: 34089–34095. [PubMed: 10567377]
 39. Zhang JQ, Nicoll G, Jones C, and Crocker PR 2000 Siglec-9, a novel sialic acid binding member of the immunoglobulin superfamily expressed broadly on human blood leukocytes. *J Biol Chem* 275: 22121–22126. [PubMed: 10801862]
 40. Adams OJ, Stanczak MA, von Gunten S, and Laubli H 2017 Targeting sialic acid-Siglec interactions to reverse immune suppression in cancer. *Glycobiology*.
 41. Choi BS, Sondel PM, Hank JA, Schalch H, Gan J, King DM, Kendra K, Mahvi D, Lee LY, Kim K, and Albertini MR 2006 Phase I trial of combined treatment with ch14.18 and R24 monoclonal antibodies and interleukin-2 for patients with melanoma or sarcoma. *Cancer Immunol Immunother* 55: 761–774. [PubMed: 16187086]
 42. Lee FT, Rigopoulos A, Hall C, Clarke K, Cody SH, Smyth FE, Liu Z, Brechbiel MW, Hanai N, Nice EC, Catimel B, Burgess AW, Welt S, Ritter G, Old LJ, and Scott AM 2001 Specific localization, gamma camera imaging, and intracellular trafficking of radiolabelled chimeric anti-G(D3) ganglioside monoclonal antibody KM871 in SK-MEL-28 melanoma xenografts. *Cancer Res* 61: 4474–4482. [PubMed: 11389078]
 43. Soiffer RJ, Chapman PB, Murray C, Williams L, Unger P, Collins H, Houghton AN, and Ritz J 1997 Administration of R24 monoclonal antibody and low-dose interleukin 2 for malignant melanoma. *Clin Cancer Res* 3: 17–24. [PubMed: 9815532]
 44. Bajorin DF, Chapman PB, Wong G, Coit DG, Kunicka J, Dimaggio J, Cordon-Cardo C, Urmacher C, Dantes L, Templeton MA, and et al. 1990 Phase I evaluation of a combination of monoclonal antibody R24 and interleukin 2 in patients with metastatic melanoma. *Cancer Res* 50: 7490–7495. [PubMed: 2253196]
 45. Alpaugh RK, von Mehren M, Palazzo I, Atkins MB, Sparano JA, Schuchter L, Weiner LM, and Dutcher JP 1998 Phase IB trial for malignant melanoma using R24 monoclonal antibody, interleukin-2/alpha-interferon. *Med Oncol* 15: 191–198. [PubMed: 9819796]
 46. Lo AS, Ma Q, Liu DL, and Junghans RP 2010 Anti-GD3 chimeric sFv-CD28/T-cell receptor zeta designer T cells for treatment of metastatic melanoma and other neuroectodermal tumors. *Clin Cancer Res* 16: 2769–2780. [PubMed: 20460472]
 47. Yun CO, Nolan KF, Beecham EJ, Reisfeld RA, and Junghans RP 2000 Targeting of T lymphocytes to melanoma cells through chimeric anti-GD3 immunoglobulin T-cell receptors. *Neoplasia* 2: 449–459. [PubMed: 11191112]

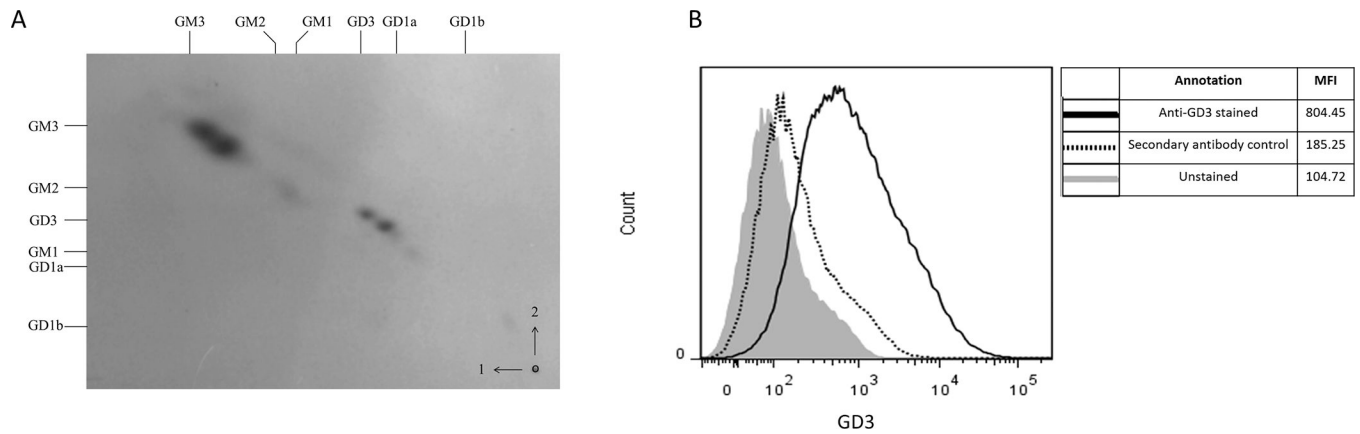
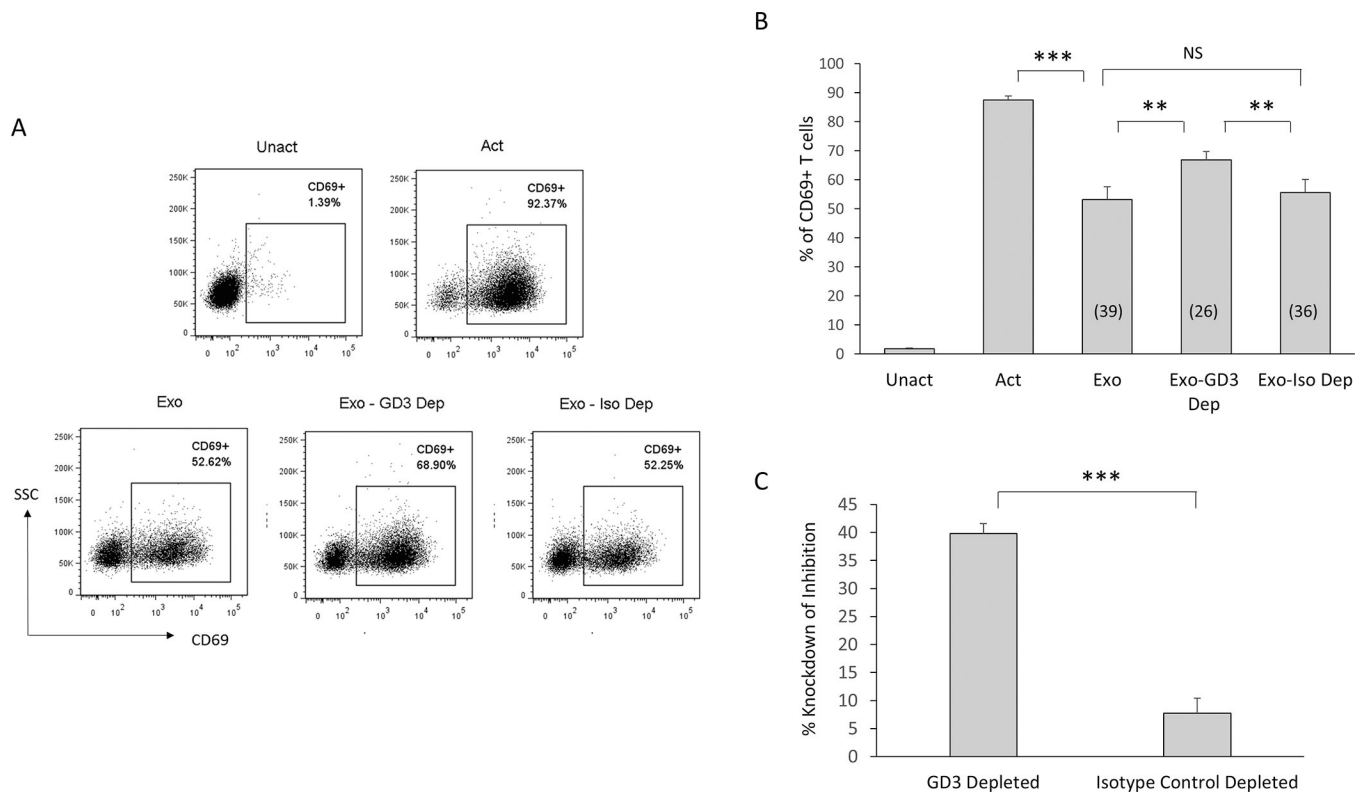
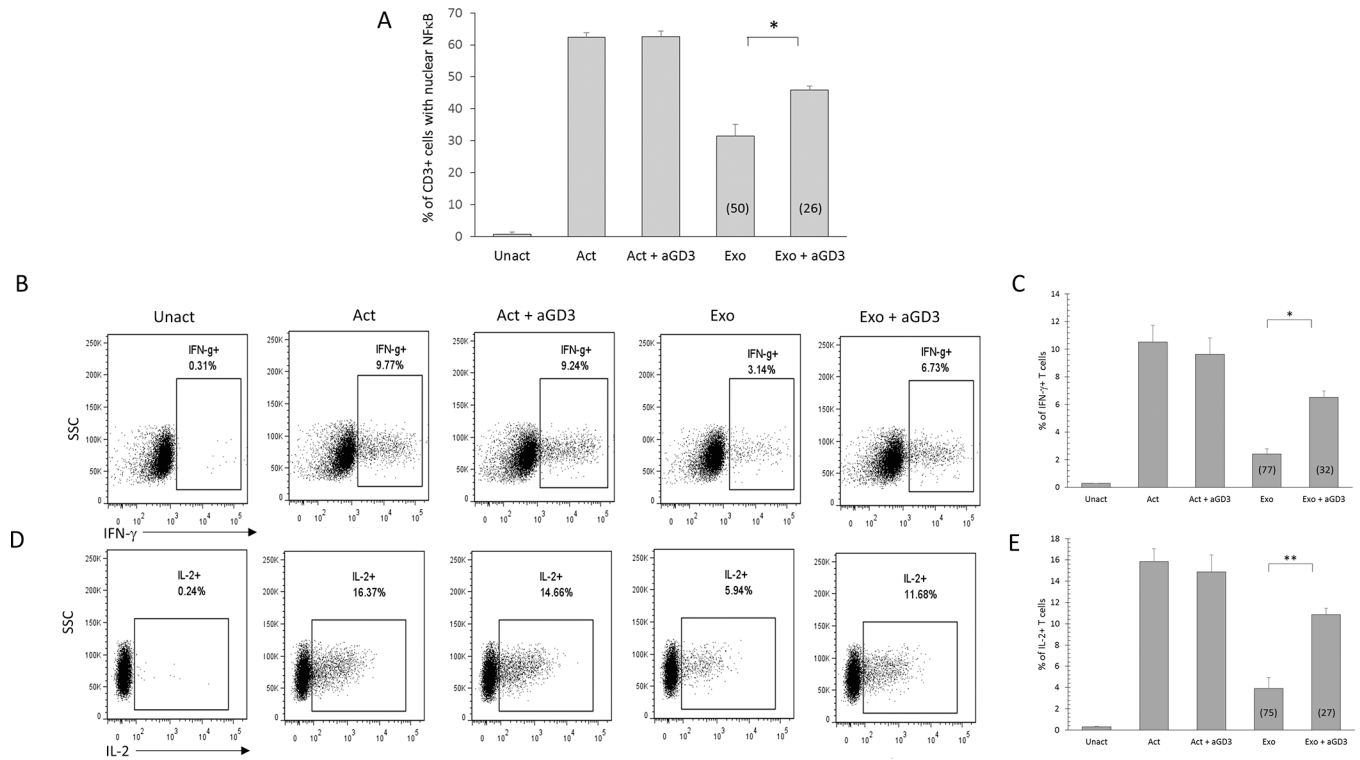


Figure 1.

Exosomes derived from ascites fluid of ovarian cancer patients express GD3 on their surface. **(A)** 2-D TLC was used to identify gangliosides GD3 and GM3 in ascites fluids. Arrows and numbers (right lower corner) indicate the directions of first and second solvent runs. Origin is in the lower right. Ganglioside standards, noted along the top (solvent 1) and left (solvent 2) margins, are: GM1 ($\text{II}^3\text{NeuAc-GgOse}_4\text{Cer}$); GD1a ($\text{IV}^3\text{NeuAc,II}^3\text{NeuAc-GgOse}_4\text{Cer}$); GD1b ($\text{II}^3(\text{NeuAc})_2\text{-GgOse}_4\text{Cer}$); GT1b ($\text{IV}^3\text{NeuAc-II}^3(\text{NeuAc})_2\text{-GgOse}_4\text{Cer}$). Standards on the right margin include GM3 ($\text{II}^3\text{NeuAc-LacCer}$); GM2 ($\text{II}^3\text{NeuAc-GgOse}_3\text{Cer}$); GM1; GD3 ($\text{II}^3(\text{NeuAc})_2\text{-LacCer}$); GD1a; GD1b. **(B)** Exosomes were attached to latex beads and either left unstained (filled histogram), labeled with secondary antibody only (dotted line) or with anti-GD3 antibody (solid line) and data acquired using a flow cytometer. Data are representative of 3 independent experiments.

**Figure 2.**

Immunodepletion of GD3⁺ exosomes diminishes exosome-mediated T cell arrest. **(A)** NDPBL were either left unactivated (Unact) or activated for 2h with immobilized antibodies to CD3 and CD28 in media only (Act) or in media with total exosomes (Exo) or exosomes subjected to depletion using either anti-GD3 antibody coupled magnetic beads (GD3 Dep) or isotype control coupled magnetic beads (Iso Dep). Activation was determined by monitoring the upregulation of CD69 on live T cells by flow cytometry following overnight incubation. Representative experiment shown. **(B)** Compiled data from 5 experiments is shown. Numbers in parentheses indicate % inhibition. **(C)** Calculated % knockdown of inhibition is shown. Mean \pm SEM. NS = Not significant ($p > 0.05$). * $p < 0.05$, ** $p < 0.01$, *** $p < 0.001$.

**Figure 3.**

Antibody-mediated blockade of ganglioside GD3 diminishes exosome-mediated immunosuppression. NDPBL were either left unactivated (Unact) or activated with immobilized antibodies to CD3 and CD28 in media without (Act) or with exosomes (Exo) derived from ovarian tumor ascites fluid in the presence or absence of 10 mg of anti-GD3 antibody. Activation was monitored by determining nuclear translocation of NFkB in CD3+ cells after 2 hours by confocal microscopy (A) or intracellular IFN-g or IL-2 expression in CD3+ cells after 6 hours by flow cytometry (B-E). Representative experiment shown for IFN-g (B) and IL-2 (D). Mean \pm SEM from 3 independent experiments shown for IFN-g (C) and IL-2 (E). Percentage inhibition is shown in parentheses. * $p < 0.05$, ** $p < 0.01$, *** $p < 0.001$.

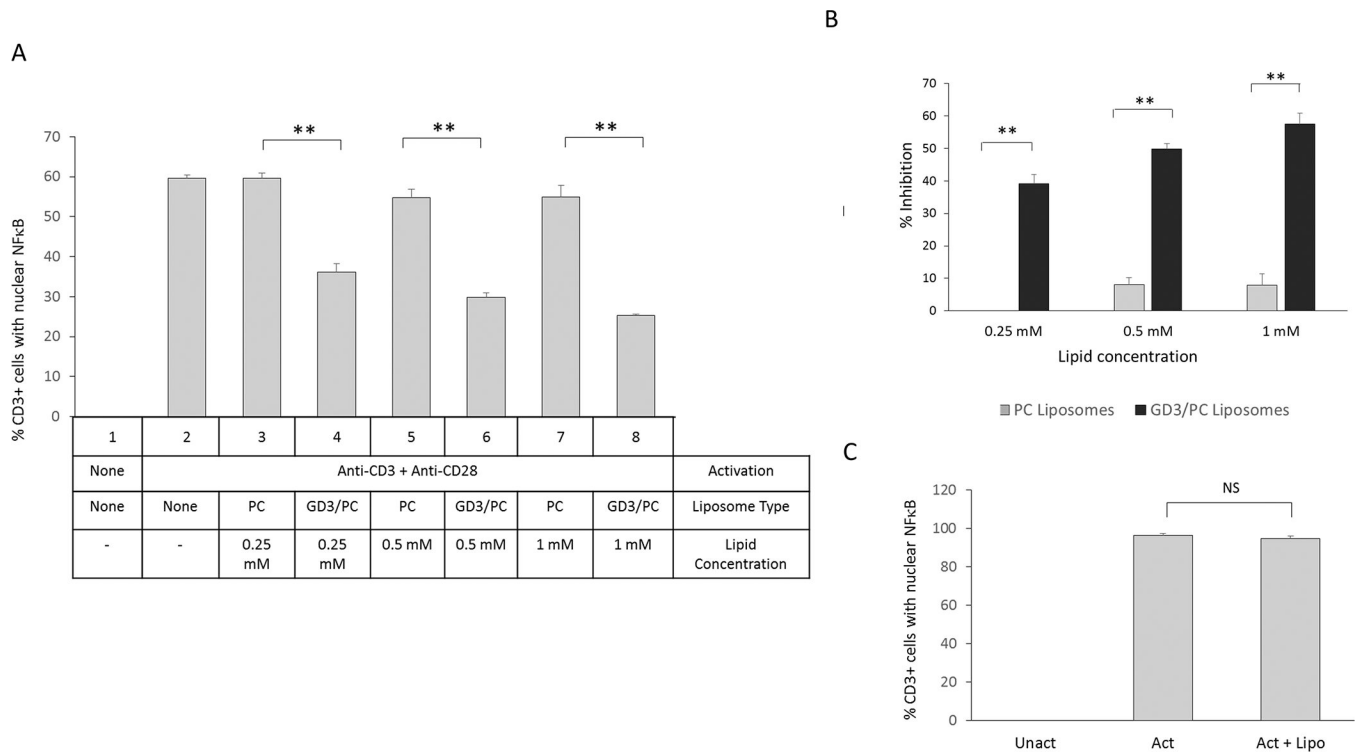


Figure 4.

GD3 liposomes arrest activation of T cell through the TCR in a dose dependent manner. **(A)** NDPBL were either left unactivated or activated for 2h with immobilized antibodies to CD3 and CD28 with various doses of PC or GD3/PC on liposomes. Activation was determined by counting the number of CD3+ cells with nuclear NFκB using confocal microscopy. **(B)** Percentage inhibition is shown. **(C)** NDPBL were either left unactivated or activated for 2h with PMA and ionomycin with 1 mM GD3/PC on liposomes. Activation was determined by counting the number of CD3+ cells with nuclear NFκB using confocal microscopy. Percentage inhibition is shown in parentheses. Mean \pm SEM; n =3. NS = Not significant ($p > 0.05$) Mean \pm SEM; n =3. ** $p < 0.01$

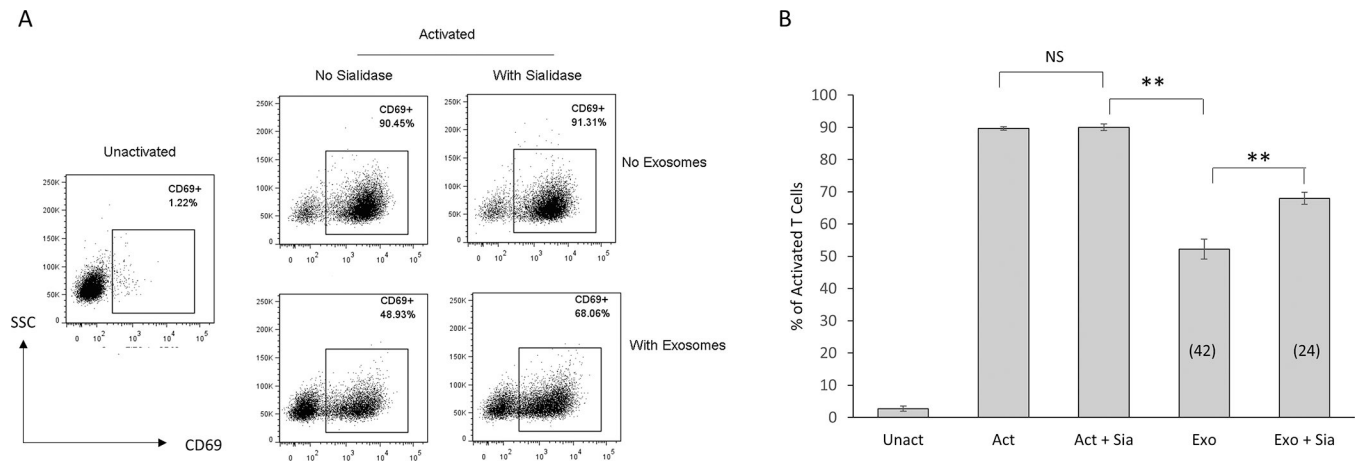


Figure 5.

Sialidase treatment of exosomes knocks down T cell arrest. NDPBL were either left unactivated (Unact) or activated for 2h with immobilized antibodies to CD3 and CD28 in media only (Act) or in media with exosomes that were untreated (Exo) or treated with 0.8 U/mL sialidase (Exo + Sia). A control group was also included where the cells were activated in the presence of the same concentration of sialidase without any exosomes present (Act + Sia). Activation was determined by monitoring the upregulation of CD69 on live T cells by flow cytometry following overnight incubation. **(A)** Representative experiment shown. **(B)** Compiled data from 5 experiments is shown. Numbers in parentheses indicate % inhibition. There was a 42% knockdown of the T cell arrest. Mean \pm SEM. $n = 3$. NS = Not significant ($p > 0.05$), ** $p < 0.01$.

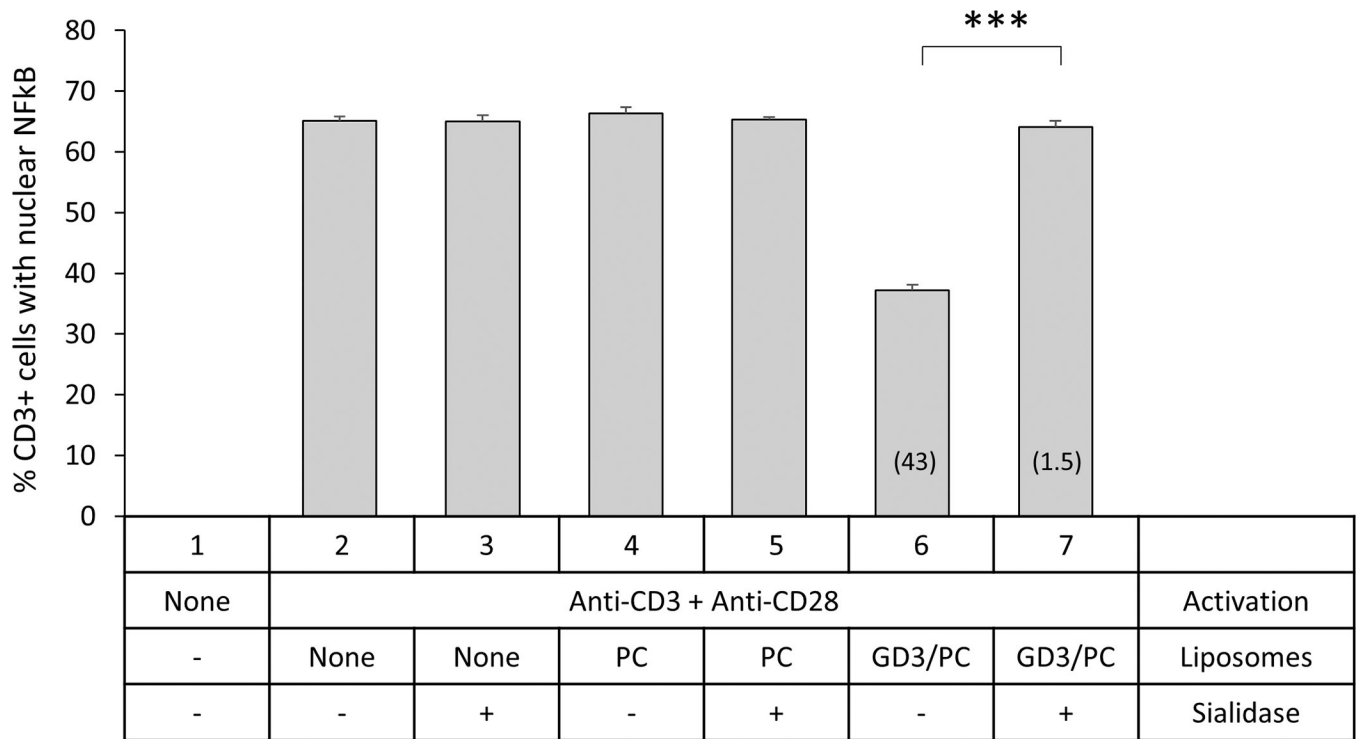


Figure 6.

Sialidase treatment of GD3 liposomes knocks down T cell arrest. NDPBL were either left unactivated or activated for 2h with immobilized antibodies to CD3 and CD28 in media only or in the presence of 1 mM PC or GD3/PC on liposomes that were untreated or treated with 0.8 U/mL sialidase. A control group was also included where the cells were activated in the presence of the same concentration of sialidase without any liposomes present. Activation was determined by counting the number of CD3+ cells with nuclear NFκB using confocal microscopy. Compiled data from 3 experiments is shown. There was a 97% knockdown of the T cell arrest. Mean ± SEM. n = 3. NS = Not significant (p > 0.05), ***p = 0.001.